Nuclear Medicine and Biology 58 (2018) 1–7

Contents lists available at ScienceDirect

Nuclear Medicine and Biology

journal homepage: www.elsevier.com/locate/nucmedbio

^{89}Zr for antibody labeling and in vivo studies – A comparison between liquid and solid target production

Gemma M. Dias [a,1], Caterina F. Ramogida [b,1], Julie Rousseau [a], Nicholas A. Zacchia [b,c], Cornelia Hoehr [b], Paul Schaffer [b,d,e], Kuo-Shyan Lin [a,d,f], François Bénard [a,d,f,*]

[a] Department of Molecular Oncology, BC Cancer Agency, Vancouver, BC, Canada
[b] Life Sciences Division, TRIUMF, Vancouver, BC, Canada
[c] Department of Chemical and Biological Engineering, University of British Columbia, Vancouver, BC, Canada
[d] Department of Radiology, University of British Columbia, Vancouver, BC, Canada
[e] Department of Chemistry, Simon Fraser University, Burnaby, BC, Canada
[f] Department of Functional Imaging, BC Cancer Agency, Vancouver, BC, Canada

ARTICLE INFO

Article history:
Received 14 July 2017
Received in revised form 10 October 2017
Accepted 15 November 2017

Keywords:
Zirconium-89
Liquid target
Radioimmunoimaging
Positron emission tomography

ABSTRACT

Introduction: Zirconium-89 (^{89}Zr, $t_{1/2}$ = 78.4 h) liquid target (LT) production offers an approach to introduce this positron-emitting isotope to cyclotron centres without the need for a separate solid target (ST) production set up. We compared the production, purification, and antibody radiolabeling yields of ^{89}Zr-(LT) and ^{89}Zr-(ST), and assessed the feasibility of ^{89}Zr-(LT) for preclinical PET/CT.

Methods: ^{89}Zr-(ST) production was performed with an ^{89}Y foil on a TR 19 cyclotron at 13.8 MeV. For LT production; an aqueous solution of yttrium nitrate ($Y(NO_3)_3 \cdot 6H_2O$) was irradiated on a TR 13 cyclotron at 12 MeV. ^{89}Zr was purified from the ST or LT material with hydroxamate resin, and used to radiolabel *p*-SCN-Bn-Deferoxamine (DFO)-conjugated Trastuzumab. MicroPET-CT imaging was performed at 1, 3 and 5 days post-injection of ^{89}Zr-DFO-Trastuzumab from ST or LT with biodistribution analysis on day 5.

Results: Irradiation of the ST yielded 2.88 ± 1.07 GBq/μA with a beam current of 14.0 ± 3.8 μA and irradiation time of 137 ± 48 min at end of bombardment while LT yielded 0.27 ± 0.05 GBq/μA with a beam current of 9.9 ± 2.2 μA and irradiation time of 221 ± 29 min. Radiolabeling of DFO-Trastuzumab with ^{89}Zr-(ST) or ^{89}Zr-(LT) was successful with purity > 97% and specific activity > 0.12 MBq/μg (of antibody). MicroPET-CT imaging and biodistribution profiles showed similar uptake of ^{89}Zr-(ST)-DFO-Trastuzumab and ^{89}Zr-(LT)-DFO-Trastuzumab in tumor and all organs of interest.

Conclusion: ^{89}Zr-(LT) was effectively used to prepare antibody bioconjugates with specific activities suitable for small animal imaging. PET imaging and biodistribution revealed similar behaviours between bioconjugates labeled with ^{89}Zr produced from the two target systems.

Advances in knowledge and implications for patient care: These results have important implications for the production of PET isotopes such as ^{89}Zr to cyclotron facilities with only LT capabilities – such as most clinical centres – expanding the availability of ^{89}Zr-immunoPET.

1. Introduction

Given its favourable decay properties (β^+ yield 23%, $E_{\beta+\,avg}$ = 396 keV; $t_{1/2}$ = 78.4 h), zirconium-89 (^{89}Zr) is rapidly gaining interest as a valuable radionuclide for immunoconjugate positron emission tomography (PET) imaging [1,2]. Most notably, the radiological half-life of ^{89}Zr matches well with the long circulation and biological half-life of antibodies, while the low energy positron decay results in high resolution making it an attractive isotope for clinical and pre-clinical use [2–7]. The production of ^{89}Zr can be accomplished on most modern medical cyclotrons, and is relatively straight-forward to pursue. Production requires targets of naturally abundant, inexpensive starting material yttrium-89 (^{89}Y) [2,8], with purification methods for ^{89}Zr also well established. A variety of methods have been developed to further improve purification efficiency and are amenable to automation [8,9].

Current production of ^{89}Zr utilizes ^{89}Y in the form of foils or pellets which are sputtered or deposited onto a solid target (ST) backing plate. The energy requirement for the ^{89}Y(p,n)^{89}Zr reaction enables sufficient yields of ^{89}Zr using low energy clinical cyclotrons to conduct pre-clinical or clinical imaging studies [10,11]. However, dissolution of the

* Corresponding author at: 675 West 10th Ave. 14-111, Vancouver, BC V5Z 1L3, Canada.
E-mail address: fbenard@bccrc.ca (F. Bénard).
[1] These authors contributed equally to the work presented.

https://doi.org/10.1016/j.nucmedbio.2017.11.005
0969-8051/

solid yttrium foil results in an exothermic reaction and generation of hydrogen gas, which requires a well-designed closed system for this dissolution process. An observation has been reported by others [12], requiring the need of a dissolution system to contain the evolved hydrogen gas from contaminating the hot cell with radioactive particles. Once dissolved and in solution, the purification of ^{89}Zr from the ^{89}Y target material can be achieved on a solid phase with a hydroxamate resin [8]. Purification of ST ^{89}Zr is typically complete within 1 h of dissolution of the irradiated material and is purified in a final solution of 1 M oxalic acid. While the ST approach is advantageous for obtaining high production yields, high operational costs and a dedicated solid target system are required to implement this technology [9]. This limits ^{89}Zr production capabilities to cyclotron facilities equipped with a dedicated solid target system. Radiolabeling of antibodies with ^{89}Zr is achievable for both clinical and pre-clinical research yielding bioconjugates with high radiochemical purity and suitable specific activity [13–16].

Producing radiometals via a liquid target (LT) system could significantly expand the availability of medically relevant radioisotopes and accelerate clinical development by leveraging the existing infrastructure in place for clinical fluorine-18 (^{18}F) production. Most recently, our group [17,18] and others [19,20] have reported the liquid target production of PET radioisotopes such as ^{44}Sc, ^{89}Zr, ^{68}Ga, and ^{86}Y. Production yields of ^{89}Zr via LT systems have been reported previously [17] with production limited by target density, but also by target performance with concerns around concomitant gas formation and pressure increases during irradiation [9]. Purification of ^{89}Zr-(LT) uses the same procedures used for ^{89}Zr-(ST); with automated delivery of the irradiated solution to a hot cell. Most notably, LT production of ^{89}Zr eliminates the need for solid target dissolution, making for a simpler post irradiation process. Advances in radiometal production via an LT system have demonstrated some improvements with yield [19]. Bansal et al. has previously showed the feasibility of preclinical PET imaging of ^{89}Zr-(LT) labeled cells [21]; however, radiolabeling efficiency of the purified isotopes for pre-clinical immunoconjugate imaging has not been assessed. The radiolabeling efficiency of radionuclides to immunoconjugates is of particular importance because it is known that the specific activity and amount of antibody injected into pre-clinical and clinical subjects can affect the biodistribution [6,22]. Successful ^{89}Zr radiolabeling of antibodies with ideal specific activity of ~0.074 MBq/μg has been achieved and assessed with conventional ^{89}Zr-(ST) production for both pre-clinical and clinical imaging [6,15,16].

Our group [17] and others [9,19] have demonstrated the feasibility of producing ^{89}Zr via a LT system. Herein we describe the feasibility of using LT produced ^{89}Zr for radiolabeling and in vivo diagnostic PET imaging of an immunoconjugate. In addition to comparing the production and purification yields of ^{89}Zr-(LT) or ^{89}Zr-(ST), we compare the radiolabeling yields, specific activity and in vivo biodistribution of an immunoconjugate, *p*-SCN-Bn-Deferoxamine-Trastuzumab (DFO-Trastuzumab), radiolabeled with ^{89}Zr produced either via the LT or ST systems.

2. Materials and methods

2.1. Reagents and instruments

The liquid target material $^{nat}Y(NO_3)_3 \cdot 6H_2O$ (99.9%) was purchased from Alfa Aesar (Ward Hill, MA, USA). ^{89}Y metal foils (99.9%, 0.254 mm thickness) were purchased from American Elements (Los Angeles, CA, USA). Ultrapure HCl (TraceSELECT®), and sodium oxalate (99.99% trace metal basis) were purchased from Sigma-Aldrich (Oakville, ON, Canada). Ultrapure nitric acid (TraceMetal™ grade) was obtained from Fisher Scientific (Ottawa, ON, Canada). A Millipore system (Direct-Q® 3UV with Pump, 18 MΩ cm^{-1}) provided ultrapure water. The bifunctional chelator *p*-SCN-Bn-Deferoxamine (DFO) was purchased from Macrocyclics (Dallas, TX, USA). Dimethyl sulfoxide (DMSO) used for chelator stock solutions was of molecular biology grade (>99.9%) obtained from Sigma-Aldrich. All other chemicals were analytical grade and used without further purification.

The radiolabeling of bioconjugates was monitored using silica-impregnated instant thin-layer chromatography paper (iTLC-SG) (Agilent Technologies, Santa Clara, CA, USA) and analyzed on a Ray Test miniGita with Beta GMC detector radio-TLC plate reader using TLC control Mini Ginastar software (Straubenhardt, Germany). After conjugation and radiolabeling respectively, 50 kDa molecular weight cut off filters (Amicon ultracentrifuges, Ultracel-50: regenerated cellulose, Millipore Corp., Billerica, MA, USA) and GE Life Sciences PD-10 desalting columns (GE, United Kingdom, MW < 5000 Da filter) and were used for purification. High performance liquid chromatography (HPLC) analyses of purified ^{89}Zr-DFO-Trastuzumab were carried out using a size-exclusion chromatography (SEC) column (Phenomenex, BioSep-SEC-s-3000) on an Agilent™ system equipped with a model 1200 quaternary pump, a model 1200 UV absorbance detector (set at 280 nm), and a Bioscan (Washington, DC, USA) NaI scintillation detector. The radiodetector was connected to a Bioscan B-FC-1000 flow-count system, and the output from the Bioscan flow-count system was fed into an Agilent 35900E interface, which converted the analog signal to a digital signal. The HPLC buffer was an isocratic gradient of 0.1 M sodium phosphate monobasic dihydrate, 0.1 M sodium phosphate dibasic dodecahydrate, 0.1 M sodium azide and 0.15 M sodium chloride (pH 6.2–7.0).

Radionuclidic purity of the irradiated salt solutions was determined by gamma spectroscopy using a Canberra Inc. (Meriden, CT, USA) N-type Co-axial high-purity germanium detector (HPGe) calibrated for energy and efficiency. After mixing, small aliquots (5–100 μL) of the irradiated solutions were removed and diluted in a standard volume of water (20 mL) for measurement; samples were measured for 30 min, and a dead time < 5%. Radioisotopic dilution, immunoreactivity and biodistribution samples were counted on a Perkin Elmer (Waltham, MA, USA) Wizard 2 2480 automated gamma counter.

2.2. Target preparation

2.2.1. Preparation of liquid target solutions

Yttrium(III) nitrate solutions were prepared as previously described [17]. Briefly, $^{nat}Y(NO_3)_3 \cdot 6H_2O$ (37.5 g) was dissolved in ultrapure water (22.7 g) and concentrated nitric acid (2.30 mL) by stirring at 40 °C overnight to give Y-nitrate in ~0.8 M HNO_3 (density = 1.48 ± 0.01 g/mL, metal concentration = 0.203 ± 0.002 g/cm^3).

2.2.2. Preparation of solid target

Yttrium foils were water jet cut into 10 mm diameters (0.089 ± 0.002 g), sandwiched between an aluminum ring and backing and loaded on a modified solid target holder based on the work of Zeisler [23].

2.3. Cyclotron target and irradiation

2.3.1. Liquid target

Experiments were performed on TRIUMF's TR13 cyclotron (Vancouver, BC, Canada; Advanced Cyclotron Systems Inc., Richmond BC, Canada), a 13 MeV self-shielded, negative hydrogen ion cyclotron. Irradiations were performed in a siphon niobium-body target with an internal target volume of 1.48 mL and an expansion chamber with a volume of 1.77 mL. The target was designed in consideration of work performed by Stokely [24]. The beam window used was a 38 μm thick Havar® foil (Goodfellow Corporation Coraopolis, PA, USA). The oval shaped target chamber was irradiated in the bottom half with a circularly collimated Gaussian beam 10 mm wide, while the top half and the expansion chamber were sufficient in volume to accommodate produced gases caused by radiolysis. Loading and unloading of the target was performed using an automated system. The target chamber was filled with solution from the bottom using a syringe pump. A bolus detector positioned past the target chamber at the top was used to verify that

the target chamber had been filled. This routinely required pushing approximately 6.2–6.5 mL of solution into the system. Once the bolus detector had tripped, an additional 1 mL of solution was pushed into the system to act as a flush upon unloading of the target. After the target chamber was loaded, the expansion chamber was pressurized with 300 to 350 psi pressure helium in order to increase the boiling point and consequently to reduce the pressure rise. All valves to the target were then shut in preparation for irradiation. The target and loading system used for these experiments have been previously described [18,25]. The irradiations were performed in several replicates using proton beams of approximately 10 μA for 60 or 240 min. Initial runs were irradiated for 60 min and increased for in vivo studies. The target solution was unloaded with pressurized helium and collected into a vial in a nearby hot cell. This unloading procedure resulted in target solution volumes of 5–7 mL.

2.3.2. Solid target irradiation

Irradiation of solid target production of ^{89}Zr was achieved on a TR19 cyclotron (Advanced Cyclotron Systems Inc.) at the BC Cancer Agency (BCCA), Vancouver, BC, Canada. The nose-piece of the target mounts into the solid target station on the cyclotron perpendicular to the beam. A vacuum is situated between the beam and a double havar foil window that allows for helium cooling. The yttrium target sits in the support ring and is cooled with water on the back of the aluminum piece. The proton beam energy was 13.8 MeV with a beam current of 14 μA on the ^{89}Y foil target. Irradiation beam time was adjusted to match experimental requirements and operational constraints and the integrated current varied.

2.4. Separation chemistry

The hydroxamate resin used for the purification of liquid or solid target ^{89}Zr was prepared as described by Holland et al. [8]. Before ^{89}Zr purification, the hydroxamate resin was packed between two frits in a 4 mL reservoir and activated with acetonitrile (8 mL), washed with ultrapure H_2O (15 mL) and conditioned with 2 M HCl (4 mL).

The irradiated ST was dissolved in 6 M HCl (2 mL) in a closed system for 1 h. The irradiated LT solution was purified at least 1 h post end of beam for 1 h irradiations or 4 h post end of beam for 4 h irradiations to reduce the radiation exposure to the experimenter derived from the amount of ^{13}N and ^{11}C coproduced during the irradiation. The ^{89}Zr solutions were diluted to 2 M HCl by adding 4 mL of H_2O for the ST; 1.4 mL of 10 M HCl was added to the LT with a further addition of 2 M HCl (5 mL). ST and LT solutions were loaded onto the conditioned hydroxamate resins of 100 and 50 mg, respectively. Once the ^{89}Zr was trapped the resins were washed with 2 M HCl (10 mL) to further remove any ^{89}Y and other impurities; subsequently washed with H_2O (10 mL) and air dried. The ^{89}Zr was eluted from the resins with 1.0 M oxalic acid in aliquots of 0.5 mL.

2.5. Trastuzumab bioconjugation

Trastuzumab (Genentech, San Francisco, CA) was purified to remove α-α-treholase dehydrate, L-histadine, and polysorbate 20 additives using centrifugal filter units with a 50 kDa molecular weight cut off and washed with PBS (pH 7.4, 15 mL) at 4000 g for 20 min four times. The final spin was washed with PBS (pH 8.9–9.1, 15 mL). Following a similar procedure to Vosjan et al. [15], purified Trastuzumab (2 mg, 13.3 nmol) was incubated with *p*-SCN-Bn-Deferoxamine (DFO, 60.23 μg, 80 nmol) at room temperature overnight with a DFO:Trastuzumab molecular ratio of 6:1 in PBS pH 8.9–9.1 in a total reaction volume of 1 mL. Conjugated DFO-Trastuzumab was then purified using the centrifugal filter technique described above and washed once with 5 mg/mL 2,5-dihydrobenzoic acid, in 0.25 M sodium acetate solution.

2.6. Optimization of ^{89}Zr antibody radiolabeling

Varying quantities (50 or 200 μL) of ^{89}Zr-oxalate were incubated with either 22.5 or 90 μL of 2 M Na_2CO_3 to adjust the pH of the ^{89}Zr to pH 6.5–7.5 at room temperature for 3 min. To this neutralized ^{89}Zr solution, DFO-Trastuzumab (50, 200 or 500 μg) was added and the volume adjusted to obtain at least a concentration of 0.2 μg/μL of DFO-Trastuzumab with PBS (pH 7.4). The reaction was allowed to progress for 60 min at room temperature, and radiolabeling yield of the reaction was assessed on iTLC-SG using 50 mM DTPA (pH 7) as mobile phase and counted on a TLC plate reader. For optimization experiments, specific activity was estimated based on radiochemical yield from iTLC results. For complete radiolabeling analysis, the ^{89}Zr-DFO-Trastuzumab was purified using size exclusion PD-10 desalting columns with PBS pH 7.4 and concentrated using 50 kDa molecular weight cut off filters. Specifically, for the in vivo study; 200 μL of ^{89}Zr-(ST) or ^{89}Zr-(LT) corresponding to 78.4 and 42.4 MBq, respectively, were neutralized with 90 μL 2 M Na_2CO_3 and incubated with 200 μg of DFO-Trastuzumab, the final volume was adjusted to 1.0 mL with PBS. Final radiochemical purity and specific activity were determined using size–exclusion HPLC.

2.7. Chelate number

The number of accessible DFO chelates conjugated to Trastuzumab was determined by radiometric isotopic dilution assays as described by Deri et al. [14]. Briefly, a stock solution of 1.4 mM $ZrCl_4$ in 1 M oxalic acid was prepared. Approximately 400 μCi of ^{89}Zr (200 μL, in 1 M oxalic acid) was added to 200 μL of the stock 'cold' Zr^{4+} solution. This ^{89}Zr[*Zr*] mixture was neutralized to pH 7 with 2 M Na_2CO_3, 1 M oxalic acid, and PBS pH 7.4 to create a working solution with a final Zr^{4+} concentration of 0.23 mM. Triplicate solutions of DFO-Trastuzumab were prepared by pipetting 30 μL of antibody in PBS (48 μg, 0.3 nmol). Negative controls using 30 μL of PBS were also prepared in triplicate. Aliquots of 20, 25, and 30 μL of the ^{89}Zr[*Zr*] working solution were added to each tube containing DFO-Trastuzumab or PBS. The solutions were incubated at room temperature with gentle mixing overnight, and subsequently quenched with a volume of 50 mM DTPA (pH 7) equal to 1/9 of the reaction volume. The reaction mixture was left to incubate for 15 min to scavenge any non-specifically bound Zr^{4+}. Each reaction was then analyzed by iTLC-SG as previously described. Strips were cut in half, each placed separately in test tubes, and counted on the calibrated gamma counter to determine the extent of radiolabeling. The average number of chelates per antibody was calculated using by dividing the cpm of the bound ^{89}Zr ($Rf = 0$) by the cpm of the unbound ^{89}Zr ($Rf > 0.5$) and multiplying that by the number of moles (n) of free Zr^{4+} divided by moles of DFO-Trastuzumab.

2.8. In vitro immunoreactivity assay

Immunoreactivity fractions of radiolabeled Trastuzumab with ^{89}Zr either from the ST or the LT were determined per the Lindmo cell-binding assay [26] using a previously established protocol [27]. Briefly, HER2-positive SKOV-3 cells were suspended at different concentrations (0.4 to 4.5 × 10^6 cells/mL in PBS). Either ^{89}Zr-(ST)-DFO-Trastuzumab or ^{89}Zr-(LT)-DFO-Trastuzumab (diluted in 1% PBS-BSA at 0.5 MBq/mL) were added to each tube in triplicates. After 1 h incubation at ambient temperature and under gentle agitation, cells were centrifuged and washed twice with PBS. The bound and unbound fractions of the radiolabeled antibodies were determined for each sample using a gamma counter (with background and decay correction). Immunoreactive fractions were estimated by linear regression analysis of total/bound activity against 1/[cell concentration].

2.9. ^{89}Zr-DFO-Trastuzumab PET/CT imaging studies

All animal experiments were performed at the Animal Resource Centre of the BC Cancer Agency Research Centre in accordance with the institutional guidelines of the University of British Columbia Animal Care Committee (Vancouver, BC, Canada) and under the supervision of authorized investigators.

Female immunodeficient NOD.Cg-Prkdc^{scid} Il2rg^{tm1Wjl}/SzJ(NSG) mice (obtained from an in-house breeding colony) were subcutaneously injected with 8×10^6 SKOV-3 cells in matrigel (BD Bioscience) on the right flank. Mice were anesthetized with isoflurane (2% in O_2) and injected via tail vein with either ^{89}Zr-(ST)-DFO-Trastuzumab (4.0 ± 0.3 MBq, corresponding to 35 ± 2 μg of antibody) or ^{89}Zr-(LT)-DFO-Trastuzumab (3.4 ± 0.2 MBq, corresponding to 22 ± 1 μg of antibody), 2 weeks after SKOV-3 cell inoculation (n = 3 per group). Each mouse underwent a CT scan for attenuation correction followed by a μPET acquisition, acquired 1, 3 and 5 days post-injection using a Siemens Inveon microPET/CT scanner (Siemens Medical Solutions, Knoxville, TN, USA) and under anesthesia (2% isoflurane-O_2). To acquire approximately the same counts for PET images the counting time was adjusted to the injected activity (20 min scan for ^{89}Zr-(ST)-DFO-Trastuzumab and 24 min scan for ^{89}Zr-(LT)-DFO-Trastuzumab). Images were reconstructed using the 3-dimensional ordered-subsets expectation maximization (OSEM3D, 2 iterations) followed by a fast maximum a priori algorithm (FastMAP: 18 iterations) and attenuation corrected based on the CT image.

2.10. Biodistribution

At day 5 post injection of the ^{89}Zr-DFO-Trastuzumab, mice were euthanized by inhalation of isoflurane followed by CO_2. Blood was withdrawn by intracardiac puncture, and then tumors and organs of interest were harvested, washed in PBS, blotted dry and weighed. Activity of each sample was measured by a gamma counter with decay correction. The activity uptake was expressed as a percentage of the injected dose per gram of tissue (%ID/g). Statistical analysis for biodistribution data were performed using GraphPad Prism (version 7). *P* values were calculated using multiple *t*-tests with the Holm-Sidak method to correct for multiple comparisons. *P* values < 0.05 were considered statistically significant.

3. Results and discussion

3.1. ^{89}Zr production

^{89}Zr-(ST) production on the TR19 was achieved with an average current of 14.6 μA, with integrated doses ranging from 631 to 2112 μA·min due to the differences in irradiation times and days. Differences in integrated currents were primarily due to the scheduling time for sufficient ^{89}Zr at the time of purification. Shorter runs (~60 min) where purification was scheduled the same or within one day of the irradiation were run with an average integrated dose of 755 ± 124 μA·min and resulted in 456 ± 116 MBq of ^{89}Zr-(ST) produced decay corrected to end of beam (EOB, n = 9). Longer irradiations, typically 130 min, where performed when purification was scheduled for at least 24 h post irradiation and were run with an average integrated dose of 1797 ± 379 μA·min and resulted in 715 ± 247 MBq ^{89}Zr decay corrected to EOB (n = 5) (Table 1).

Due to the 100% natural abundance of ^{89}Y, irradiation of the $Y(NO_3)_3$ solution in the liquid target system produced solely ^{89}Zr through the ^{89}Y(p,n)^{89}Zr reaction. A one hour irradiation of $Y(NO_3)_3$ solution produced on average 38 ± 17 MBq of ^{89}Zr (n = 9, decay corrected to EOB, Table 1); while this was a sufficient amount of activity to test radiolabeling chemistry, it is likely below the lower limit needed to prepare an antibody conjugate of high enough specific activity for a comprehensive pre-clinical imaging study. To produce sufficient yields of ^{89}Zr to complete a pre-clinical imaging study, four hour irradiations were performed. A 4 h irradiation produced an average of 85 ± 3 MBq of activity (n = 4, decay corrected to EOB, Table 1). A comparison of solid and liquid ^{89}Zr production yields found in literature are compared (Table 2). While the saturation yield of the 60 min irradiation agrees well within error with the results from Pandey et al. for an irradiation of 120 min, our longer 221 min irradiation has a lower saturation yield compared to the 60 min irradiation of 50%. While a drop in saturation yield for longer irradiation is expected [28], the magnitude of the drop is not understood at this moment. The radionuclidic purity of the crude irradiated LT solution 48 h after EOB and dissolved ST 72 h after EOB were found to be >99.0%, confirmed by gamma spectroscopy (Fig. 1).

Table 1
Summary of ^{89}Zr production parameters for solid and liquid target irradiations. Results are given as mean ± SD.

	Solid target		Liquid target	
Cyclotron	TR 19 BCCA		TR 13 TRIUMF	
Integrated dose [μA·min]	755 ± 124	1797 ± 379	639 ± 133	2159 ± 507
Number of runs	9	5	9	4
Proton energy [MeV]	13.9	13.9	12	12
Beam current [μA]	14.5 ± 4.2	14.0 ± 3.8	10.9 ± 3.0	9.9 ± 2.3
Beam time [min]	60 ± 28	137 ± 48	58 ± 4	221 ± 29
EOB Yield [MBq]	456 ± 116	715 ± 247	38 ± 17	85 ± 35
Saturated Yield [MBq/μA]	3990 ± 642	2879 ± 1074	407 ± 160	266 ± 51
Purified ^{89}Zr at EOB [MBq]	339 ± 89	507 ± 237	20 ± 13	76 ± 26

3.2. ^{89}Zr purification

Purification of the ^{89}Zr from the ^{89}Y target material was achieved with solid phase separation on a hydroxamate resin for both ST and LT productions. Extraction and purification of the ST irradiated foil was often performed at least 24 h after EOB. Due to the current set up at BCCA, manual extraction of the foil was required and performed when the field from the target was acceptable and around daily clinical ^{18}F production runs. Purification of ^{89}Zr-(ST) is achievable within 30 min after the complete dissolution of the irradiated foil, 100 mg of the hydroxamate resin. As described in the methods, the dissolved ST solution was diluted to 2 M HCl and loaded onto the resin, washed with 2 M HCl and H_2O and eluted with 0.5 mL aliquots of 1 M oxalic acid. The activity from the first 0.5 mL elution from ST purification often yielded sufficient activity required for optimizing radiolabeling conditions and for in vivo studies. On average, 57 ± 17% of radioactivity from the irradiated foil was eluted in the first 0.5 mL elution from the hydroxamate resin resulting in 281 ± 94 and 359 ± 145 MBq decayed to EOB for the lower and higher integrated dose runs respectively. Additional elutions resulted in the recovery of 71 ± 16%, with a total yield of 339 ± 89 and 507 ± 237 MBq for the lower and higher integrated dose runs in a total volume of 1.0–1.5 mL. The purified ^{89}Zr at EOB represented in Table 1

Table 2
Comparison of ^{89}Zr ST and LT production yields to literature results.

	Solid target		Liquid target	
	BCCA	Holland et al. [8]	TRIUMF	Pandey et al. [19]
Yttrium [g]	0.089	0.33	0.3	0.28
Proton energy [MeV]	13.8	15	12	14
Beam current [μA]	14.0 ± 3.8	15	9.9 ± 2.3	40
Beam time [min]	137 ± 48	145 ± 18	221 ± 26	120
EOB Yield [MBq]	715 ± 247	2044 ± 387	85 ± 35	349 ± 49
Yield [MBq/μA·h]	25.2 ± 9.4	56.1 ± 4.3	2.3 ± 0.4	4.4 ± 0.6

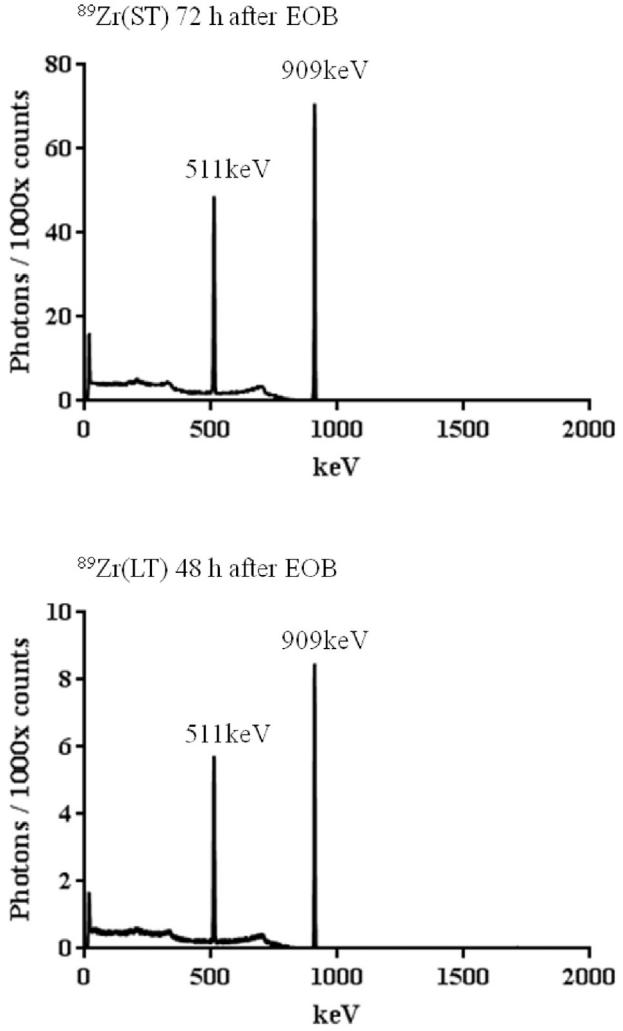

Fig. 1. Spectrums of the gamma-ray emissions observed from unpurified samples of ^{89}Zr-(ST) above and ^{89}Zr-(LT) below, acquired 72 h (ST) and 48 h (LT) post EOB.

includes the total yield from all elutions. For purification of ^{89}Zr for the in vivo study, the activity and concentration in the first elution was sufficient for radiolabeling and an additional elution was not performed.

Purification of ^{89}Zr-(LT) required the addition of 10 M HCl (1.4 mL) to the irradiated nitric acid solution with an addition of 2 M HCl (5 mL) in order to adjust the acid concentration to 2 M HCl prior to loading the solution onto a 50 mg hydroxamate resin following procedures outlined previously by our group [17]. To reduce radiation exposure due to the presence of co-produced ^{13}N and ^{11}C, purification of the LT solution started 1 or 4 h post EOB, for a 60 or 240 min irradiation, respectively. Separation efficiency of the LT solution was 91 ± 6%, resulting in 20 ± 13 MBq decay corrected to EOB for a 60 min irradiation. The elution of the final ^{89}Zr product was achieved with one 0.5 mL elution of 1 M oxalic acid. By increasing the irradiation time to 4 h, 66 ± 26 MBq of ^{89}Zr-(LT) was isolated (76 ± 26 MBq ^{89}Zr decay corrected to EOB).

3.3. Antibody radiolabeling

3.3.1. Optimization and comparison of antibody radiolabeling with ^{89}Zr-(ST) versus ^{89}Zr-(LT)

To optimize radiolabeling and to obtain specific activity (SA) suitable for in vivo μPET imaging (>0.07 MBq/μg), a range of volumes of purified ^{89}Zr-(ST) (50 or 200 μL) were neutralized with the appropriate amount of 2 M Na_2CO_3 (22.5 or 90 μL) (Table 3). To these conditions, 50 μg, 200 μg or 500 μg of conjugated DFO-Trastuzumab in PBS were added. Radiolabeling of the conjugated mAb was achieved at ambient temperatures at pH 7.0 within 1 h. Radiolabeling efficiency was assessed by iTLC and estimated SA was calculated based on the radiolabeling efficiency divided by the amount of starting DFO-Trastuzumab, this provided a crude and reasonable estimation of SA (Table 3). Initially using 200 μL of ^{89}Zr-(ST) and 200 μg of DFO-Trastuzumab, a radiolabeling yield of 37% with an estimated SA of 0.16 MBq/μg was obtained. Increasing the amount of DFO-Trastuzumab (500 μg) in the reaction increased the radiolabeling yield to 66%; however, consequently resulted in a lower SA (0.06 MBq/μg).

Table 3
Radiolabeling conditions of DFO-Trastuzumab with either ^{89}Zr-(ST) or ^{89}Zr-(LT). Radiochemical yield (RCY) determined from iTLC and estimated specific activity (SA) based on RCY and starting DFO-Trastuzumab (μg) are shown.

	Solid target (ST)			Liquid target (LT)	
^{89}Zr (μL)	200	200	50	200	50
^{89}Zr (MBq)	65	82	23	33	10
1 M oxalic acid (μL)	90	90	22.5	90	22.5
mAb [μg]	500	200	200	200	50
RCY	66%	37%	81%	51%	49%
SA [MBq/μg]	0.06	0.16	0.10	0.09	0.07

In order to compare the efficiency of radiolabeling between ^{89}Zr-(ST) and ^{89}Zr-(LT) using the similar amount of activity, the volume of ^{89}Zr-(ST) was decreased proportionally to match the activity measured in 200 μL of ^{89}Zr-(LT). Using 50 μL of ^{89}Zr-(ST) in the radiolabeling reaction further improved radiolabeling yield to 81% while SA decreased to 0.10 MBq/μg (Table 3). Nevertheless, the bioconjugate was still sufficient for imaging. Generally, lower starting volumes of ^{89}Zr-(ST)-oxalate in the radiolabeling reactions resulted in higher radiochemical yields.

When comparing the radiolabeling efficiency of DFO-Trastuzumab (200 μg) with an equal volume (200 μL) of ^{89}Zr-(LT) or ^{89}Zr-(ST) radiochemical yields using liquid target ^{89}Zr were higher (51% vs. 37% RCY respectively). This suggests that ^{89}Zr-oxalate isolated from a LT may contain lower concentrations of non-radioactive metal impurities compared to ^{89}Zr-(ST)-oxalate. Reducing both the ^{89}Zr-(LT) volume and amount of DFO-Trastuzumab in a radiolabeling reaction resulted in radioimmunoconjugates with sufficient SA for in vivo studies but not sufficient activity for μPET imaging. Radiolabeling 200 μg of DFO-Trastuzumab with 200 μL of ^{89}Zr-(LT) resulted in a RCY of 51%. Decreasing the amount of DFO-Trastuzumab to 50 μg and ^{89}Zr-(LT) (50 μL) maintained a 49% RCY. Both radiolabeling conditions resulted in suitable SAs for μPET imaging of 0.09 and 0.07 MBq/μg respectively (Table 3). As the volume to volume comparison does not take into consideration the much higher amount of ^{89}Zr activity in the ST solution; by reducing the volume of ^{89}Zr-(ST) to 50 μL to match the activity within 200 μL of ^{89}Zr-(LT), similar SAs were obtained after radiolabeling of the same quantity of antibody (Table 3).

3.3.2. Antibody radiolabeling with either ^{89}Zr-(ST) or ^{89}Zr-(LT) for in vivo study

For the in vivo study, in order to obtain the best radiolabeling potential using either ^{89}Zr-(LT) or ^{89}Zr-(ST), DFO-Trastuzumab (200 μg) was incubated with the same volume of 200 μL of ^{89}Zr (ST: 78.4 MBq, LT: 42.2 MBq) (Table 4). After 60 min, iTLC results from the crude reaction showed better radiolabeling with the ^{89}Zr-(LT) (55%) than ^{89}Zr-(ST) (33%). FollowingPD-10 purification and concentration of the radiolabeled Trastuzumab, iTLC of the final products showed 97% and 98% radiochemical purity for the ^{89}Zr-(ST) and ^{89}Zr-(LT) reactions, respectively. The predicted SA estimation based on iTLC was consistent with previous radiolabeling performed during the optimization process by size-exclusion HPLC, the SAs for ST (0.12 MBq/μg) and LT (0.15 MBq/μg) were determined and suitable for μPET imaging. The final activity of

Table 4
Radiolabeling conditions for the in vivo study of DFO-Trastuzumab with either ^{89}Zr-(ST) or ^{89}Zr-(LT). Radiochemical yield (RCY) determined from iTLC and specific activity (SA) determined based on SEC HPLC are shown.

	Solid target (ST)	Liquid target (LT)
^{89}Zr (μL)	200	200
^{89}Zr (MBq)	78.4	42.2
mAb [μg]	200	200
RCY	33%	55%
SA [MBq/μg]	0.12	0.15

purified ^{89}Zr-DFO-Trastuzumab products prepared for animal injections were: ST: 18.6 MBq and LT: 15.5 MBq. In parallel, the number of chelates per DFO-Trastuzumab and the immunoreactivity were determined. An average of 2.6 ± 0.3 DFO chelates per mAb was determined for the DFO-Trastuzumab immunoconjugate. Immunoreactive fractions within the same range were obtained (72 and 67% for ST and LT ^{89}Zr-DFO-Trastuzumab respectively).

3.4. Small animal μPET-CT imaging and biodistribution

μPET-CT images were acquired at 1, 3 and 5 days post-injection (Fig. 2) of ^{89}Zr-DFO-trastuzumab. Images showed similar high uptake of the radiolabeled immunoconjugate within the SKOV-3 tumors as early as day 1 post-injection. For ^{89}Zr-(ST)-DFO-Trastuzumab and ^{89}Zr-(LT)-DFO-Trastuzumab, a typical biodistribution profile of a radiolabeled immunoconjugate was observed with high liver, heart and spleen uptake. High contrast PET images were obtained for both, enabling clear visualization of the tumor xenografts. Also, tumor uptake increased over the 5 day period for both compounds. Notably as with most ^{89}Zr-DFO complexes in mice, demetalation of the ^{89}Zr was observed and increased over the progression of the study; evident by the qualitative increase in bone uptake.

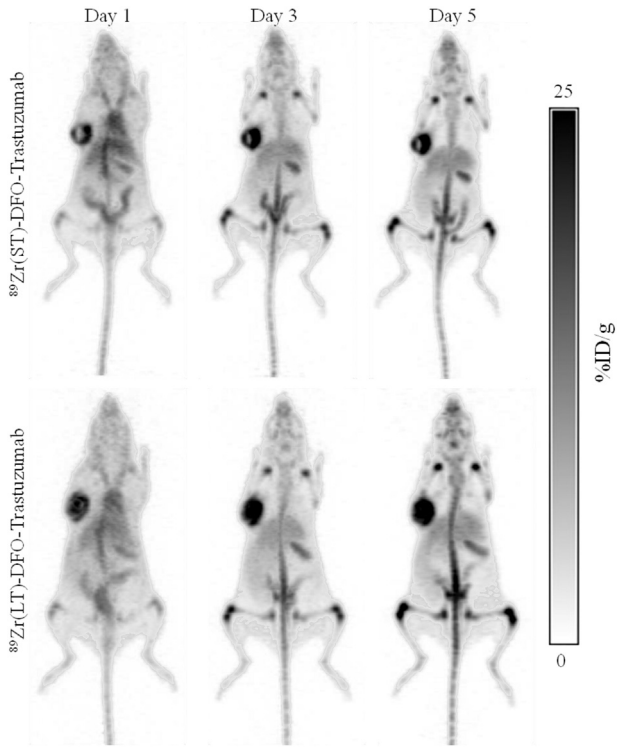

Fig. 2. Representative μPET images of DFO-Trastuzumab labeled with ^{89}Zr either from solid target (ST) or liquid target (LT). Mice were anesthetized with 2% isoflurane in O_2 and injected with ST: 4.0 MBq or LT: 3.4 MBq, and imaged for ST: 20 min, LT: 24 min at day 1, 3 and 5. Scale bar indicates %ID/g.

Biodistribution data corroborated the PET imaging results. High tumor uptake expressed as percent of injected dose per gram of tissue (%ID/g) at day 5 were statistically the same for both groups; ST: 25.22 ± 3.63%ID/g and LT: 21.66 ± 3.90%ID/g (Table 5). No statistical differences in organs of interest were noticed between the two groups. Both groups exhibited similar tumor-to-blood or tumor-to-non-target organ (liver, spleen, kidneys or heart) ratios. Imaging quality and biodistribution showed no noticeable differences suggesting ^{89}Zr-(LT) to be a suitable alternative to ^{89}Zr-(ST) for preclinical μPET imaging.

4. Conclusion

We have demonstrated production, purification and radiolabeling of antibodies using ^{89}Zr produced via a LT system. Comparing this with traditional ^{89}Zr-(ST) production, the radiolabeling of an antibody was successful with sufficient specific activities for in vivo pre-clinical imaging. Increased irradiation time on a LT system improved the yield providing the pressure constraints on the target are respected. ^{89}Zr-(LT) demonstrated higher purification yields and improved radiolabeling yields over ST produced ^{89}Zr. Reducing the volume of ^{89}Zr-(ST)-oxalate for radiolabeling resulted in higher and comparable radiochemical yields to that of LT. One difference between the ST and LT was a higher radiolabeling yield with the LT solution. Radiolabeling of DFO-Trastuzumab was successful with both ^{89}Zr-(ST) and ^{89}Zr-(LT), and an optimal specific activity of radiolabeled Trastuzumab was achieved. No significant differences were observed in imaging quality or biodistribution between ST or LT ^{89}Zr-labeled immunoconjugates. Thus, LT ^{89}Zr shows promise for use in pre-clinical diagnostic imaging in cyclotron centres with only LT production set up. Further improvement to obtain higher ^{89}Zr production yields and specific activities after radiolabeling, comparable to the ones obtained with the ST approach, will be needed to make this production approach more attractive for larger studies and clinical applications.

Acknowledgments

The authors would like to thank cyclotron operators at BC Cancer Agency: Wade English, Milan Vuckovic and Julius Klug and TRIUMF: Dave Prevost, Linda Graham and Sam Varah.

Funding for this work was provided by the Canadian Institutes for Health Research (CIHR) CPG-121051 and National Sciences and Engineering Research Council of Canada (NSERC) CHRP-413841-12. TRIUMF receives funding via a contribution agreement with the National Research Council of Canada.

Table 5
Biodistribution data (%ID/g; mean ± SD) 5 days after injection of ^{89}Zr-(ST)-DFO-Trastuzumab (n = 4) or ^{89}Zr-(LT)-DFO-Trastuzumab (n = 3) in NSG mice bearing SKOV-3 tumor xenografts.

Tissues	^{89}Zr-(ST)-DFO-Trastuzumab	^{89}Zr-(LT)-DFO-Trastuzumab
Blood	1.51 ± 0.54	2.88 ± 2.01
Fat	0.56 ± 0.31	0.98 ± 0.10
Uterus	20.06 ± 8.46	11.70 ± 2.07
Ovaries	5.83 ± 0.65	6.03 ± 2.43
Intestine	3.26 ± 0.27	2.79 ± 0.52
Stomach	1.90 ± 0.22	2.07 ± 0.30
Spleen	66.74 ± 7.96	52.98 ± 9.50
Liver	8.26 ± 0.21	7.58 ± 0.96
Pancreas	1.06 ± 0.06	1.33 ± 0.29
Adrenals	3.10 ± 0.46	3.47 ± 0.22
Kidney	2.87 ± 0.07	2.53 ± 0.79
Lungs	2.77 ± 0.36	2.81 ± 0.78
Heart	1.22 ± 0.17	1.19 ± 0.43
SKOV-3 tumor	25.22 ± 3.63	21.66 ± 3.90
Muscle	0.57 ± 0.01	0.54 ± 0.13
Bone	12.11 ± 0.99	14.06 ± 0.85
Brain	0.14 ± 0.03	0.16 ± 0.05

References

[1] Chen K, Conti PS. Target-specific delivery of peptide-based probes for PET imaging. Adv Drug Deliv Rev 2010;62:1005–22.
[2] Holland JP, Williamson MJ, Lewis JS. Unconventional nuclides for radiopharmaceuticals. Mol Imaging 2010;9:1–20.
[3] Wu AM, Senter PD. Arming antibodies: prospects and challenges for immunoconjugates. Nat Biotechnol 2005;23:1137–46.
[4] Boswell CA, Brechbiel MW. Development of radioimmunotherapeutic and diagnostic antibodies: an inside-out view. Nucl Med Biol 2007;34:757–78.
[5] Dijkers EC, Munnink THO, Kosterink JG, Brouwers AH, Jager PL, de Jong JR, et al. Biodistribution of Zr-89-trastuzumab and PET imaging of HER2-positive lesions in patients with metastatic breast cancer. Clin Pharmacol Ther 2010;87:586–92.
[6] Jauw YWS, Menke-van der Houven van Oordt CW, Hoekstra OS, Hendrikse NH, Vugts DJ, Zijlstra JM, et al. Immuno-positron emission tomography with zirconium-89-labeled monoclonal antibodies in oncology: what can we learn from initial clinical trials? Front Pharmacol 2016;7:131–46.
[7] Zhang Y, Hong H, Cai W. PET tracers based on zirconium-89. Curr Radiopharm 2011;4:131–9.
[8] Holland JP, Sheh YC, Lewis JS. Standardized methods for the production of high specific-activity zirconium-89. Nucl Med Biol 2009;36:729–39.
[9] Pandey MK, Engelbrecht HP, Byrne JP, Packard AB, DeGrado TR. Production of ^{89}Zr via the ^{89}Y(p,n)^{89}Zr reaction in aqueous solution: effect of solution composition on in-target chemistry. Nucl Med Biol 2014;41:309–16.
[10] Uddin MS, Hagiwara M, Baba M, Tarkanyi F, Ditroi F. Experimental studies on excitation functions of the proton-induced activation reactions on yttrium. Appl Radiat Isot 2005;63:367–74.
[11] Mustafa MG, West HI, Obrien H, Lanier RG, Benhamou M, Tamura T. Measurements and a direct-reaction-plus-Hauser-Feshbach analysis of Y-89(P,N)Zr-89, Y-89(P,2n)Zr-89, and Y-89(P,Pn)Y-88 reactions up to 40 MeV. Phys Rev C 1988;38:1624–37.
[12] Siikanen J, Peterson M, Tran TA, Roos P, Ohlsson T, Sandell A. A peristaltic pump driven ^{89}Zr separation module. AIP conference proceedings, Vol. 1509. ; 2012. p. 206–10.
[13] Menke-van der Houven van Oordt CW, Gootjes EC, Huisman MC, Vugts DJ, Roth C, Luik AM, et al. ^{89}Zr-cetuximab PET imaging in patients with advanced colorectal cancer. Oncotarget 2015;6:30384–93.
[14] den Hollander MW, Bensch F, Glaudemans AW, Oude Munnink TH, Enting RH, den Dunnen WF, et al. TGF-beta antibody uptake in recurrent high-grade glioma imaged with ^{89}Zr-fresolimumab PET. J Nucl Med 2015;56:1310–4.
[15] Vosjan MJ, Perk LR, Visser GW, Budde M, Jurek P, Kiefer GE, et al. Conjugation and radiolabeling of monoclonal antibodies with zirconium-89 for PET imaging using the bifunctional chelate *p*-isothiocyanatobenzyl-desferrioxamine. Nat Protoc 2010;5:739–43.
[16] Verel I, Visser GW, Boellaard R, Stigter-van Walsum M, Snow GB, van Dongen GA. ^{89}Zr immuno-PET: comprehensive procedures for the production of ^{89}Zr-labeled monoclonal antibodies. J Nucl Med 2003;44:1271–81.
[17] Oehlke E, Hoehr C, Hou X, Hanemaayer V, Zeisler S, Adam MJ, et al. Production of Y-86 and other radiometals for research purposes using a solution target system. Nucl Med Biol 2015;42:842–9.
[18] Hoehr C, Oehlke E, Benard F, Lee CJ, Hou X, Badesso B, et al. (44g)Sc production using a water target on a 13 MeV cyclotron. Nucl Med Biol 2014;41:401–6.
[19] Pandey MK, Bansal A, Engelbrecht HP, Byrne JF, Packard AB, DeGrado TR. Improved production and processing of (8)(9)Zr using a solution target. Nucl Med Biol 2016;43:97–100.
[20] Pandey MK, Byrne JF, Jiang H, Packard AB, DeGrado TR. Cyclotron production of (68)Ga via the (68)Zn(p,n)(68)Ga reaction in aqueous solution. Am J Nucl Med Mol Imaging 2014;4:303–10.
[21] Bansal A, Pandey MK, Demirhan YE, Nesbitt JJ, Crespo-Diaz RJ, Terzic A, et al. Novel (89)Zr cell labeling approach for PET-based cell trafficking studies. EJNMMI Res 2015;5:19–30.
[22] Lee JH, Kim H, Yao ZS, Lee SJ, Szajek LP, Grasso L, et al. Tumor and organ uptake of Cu-64-labeled MORAb-009 (amatuximab), an anti-mesothelin antibody, by PET imaging and biodistribution studies. Nucl Med Biol 2015;42:880–6.
[23] Zeisler SK, Pavan RA, Orzechowski J, Langlois R, Rodrigue S, van Lier JE. Production of Cu-64 on the Sherbrooke TR-PET cyclotron. J Radioanal Nucl Chem 2003;257:175–7.
[24] Stokely MH. Deployment, testing and analysis of advanced thermosyphon target systems for production of aqueous fluorine-18 via oxygen-18 (p,n) fluorine-18. Raleigh, North Carolina: North Carolina State University; 2008.
[25] Zacchia NA, Martinez DM, Hoehr C. Foil degradation in a salt solution target. AIP conference proceedings, 1845. ; 2017. p. 020024.
[26] Lindmo T, Boven E, Cuttitta F, Fedorko J, Bunn PA. Determination of the immunoreactive fraction of radiolabeled monoclonal-antibodies by linear extrapolation to binding at infinite antigen excess. J Immunol Methods 1984;72:77–89.
[27] Rousseau J, Zhang Z, Dias GM, Zhang C, Colpo N, Benard F, et al. Design, synthesis and evaluation of novel bifunctional tetrahydroxamate chelators for PET imaging of ^{89}Zr-labeled antibodies. Bioorg Med Chem Lett 2017;27:708–12.
[28] Buckley KR, Huser JM, Jivan S, Chun KS, Ruth TJ. 11C-methane production in small volume, high pressure gas targets. Radiochim Acta 2000:201–6.